Marta I. Litter[1,2,3] / Mariel Slodowicz[1,2]

An overview on heterogeneous Fenton and photoFenton reactions using zerovalent iron materials

[1] División Química de la Remediación Ambiental, Gerencia Química, Comisión Nacional de Energía Atómica, Av. Gral. Paz 1499, 1650 San Martín, Prov. de Buenos Aires, Argentina, E-mail: marta.litter@gmail.com, mariels777@gmail.com
[2] Consejo Nacional de Investigaciones Científicas y Técnicas, Godoy Cruz 2290, 1425 Buenos Aires, Argentina, E-mail: marta.litter@gmail.com, mariels777@gmail.com
[3] Instituto de Ingeniería e Investigación Ambiental, Universidad de Gral. San Martín, Campus Miguelete, Av. 25 de Mayo y Francia, 1650 San Martín, Prov. de Buenos Aires, Argentina, E-mail: marta.litter@gmail.com

Abstract:
The basic and applied aspects of Fenton and Fenton-like processes for removal of pollutants using zerovalent iron materials, including nanoparticles, are reviewed in this article. Only those examples including the use of the iron materials together with hydrogen peroxide addition are included. The mechanistic aspects of homogeneous and heterogeneous Fenton processes, still under discussion, are displayed. The use of biogenic generated iron nanoparticles for removal of pollutants is discussed due to their novelty and economy of synthesis.

Keywords: Fenton, photoFenton, zerovalent iron, nanoparticles, removal of pollutants

DOI: 10.1515/jaots-2016-0164

Received: November 18, 2016; **Revised:** November 18, 2016; **Accepted:** November 28, 2016

1 Introduction

1.1 The Fenton reaction

The Fenton reagent, a mixture of hydrogen peroxide and ferrous salt, and derived Fenton-like processes have been recognized since long time as efficient processes for the treatment of organic and inorganic compounds in water (see e. g. references [1–3]. H.J.H. Fenton was the first to describe the oxidation of tartaric acid in the presence of H_2O_2 and ferrous iron ions [4]. Due to Fenton's initial research, the oxidation of organic and inorganic substrates by iron (II) and H_2O_2 is known as the Fenton reaction. The Fenton processes are, until now, one of the most effective methods for the oxidation of organic pollutants [5, 6]. Their use for the chemical degradation of industrial wastewater components such as aromatic amines [7], dyes [8–10], pesticides [11–13], surfactants [14–16], and explosives [17], among others, is very well established and rather well understood.

The Fenton process is a rather low-cost technology useful to treat wastewater with total organic carbon (TOC) contents below 15 mg L^{-1}. This process is a convenient tool to increase the biocompatibility of the effluent, as it converts most of the organic pollutants into low-molecular-mass organic acids. Even mineralization, i. e., formation of CO_2, water and small inorganic molecules, can be achieved in some cases. Generally, the working pH in Fenton processes should be around 3 to avoid the precipitation of iron oxohydroxides that can inhibit the process. In addition to pH, the H_2O_2/Fe^{2+} ratio, the temperature and the reaction time are variables affecting the efficiency of Fenton processes [5, 18–20].

1.2 Main characteristics of the Fenton reaction

1.2.1 Mechanism of the Fenton reaction

The mechanism of the Fenton reaction is still under investigation due to the uncertainty of the identity of the main involved species. Two reaction pathways have been proposed [21]. One involves the participation of free

Marta I. Litter is the corresponding author.

radicals through a chain reaction (Haber-Weiss mechanism) [22–25], and the other (Kremer-Stein mechanism) implicates an ionic mechanism through the formation of the FeO^{2+} intermediate, involving Fe(IV) [25–31], proposed first by Bray and Gorin [32].

The typical accepted reactions involved in Fenton processes according to the first chain mechanism are displayed in below [6]. Equations (1–5) display reactions of Fe^{2+} and Fe^{3+} with H_2O_2 and the subsequent intermediates in the absence of other ions and/or organic substances. Reaction of eq. (1), known as the classical Fenton reaction, is the initial step that produces the strong oxidizing radical $HO^{\bullet}$. In the process, H_2O_2 is continuously consumed during the reaction, and the iron added in small amounts serves as a catalyst [6]. The regeneration of Fe^{2+} can be achieved by continuous addition of H_2O_2 to the system, where Fe^{3+} ions are present (eq. (2)).

$$Fe^{2+} + H_2O_2 \rightarrow Fe^{3+} + HO^- + HO^{\bullet} \qquad 40 - 80\,M^{-1}s^{-1} \tag{1}$$

$$Fe^{3+} + H_2O_2 \rightarrow Fe^{2+} + HO_2^{\bullet} + H^+ \qquad 9.1 \times 10^{-7} M^{-1}\,s^{-1} \tag{2}$$

$$Fe^{2+} + HO^{\bullet} \rightarrow Fe^{3+} + HO^- \qquad 2.5 - 5 \times 10^8\,M^{-1}\,s^{-1} \tag{3}$$

$$Fe^{3+} + HO_2{}^{\bullet} \rightarrow Fe^{2+} + H^+ + O_2 \qquad 0.33 - 2.1 \times 10^6\,M^{-1}\,s^{-1} \tag{4}$$

$$Fe^{2+} + HO_2{}^{\bullet} \rightarrow Fe^{3+} + HO_2{}^- \qquad 0.72 - 1.5 \times 0^6\,M^{-1}\,s^{-1} \tag{5}$$

$$H_2O_2 + HO^{\bullet} \rightarrow HO_2{}^{\bullet} + H_2O \qquad 1.7 - 4.5 \times 0^7\,M^{-1}\,s^{-1} \tag{6}$$

$$2\,HO^{\bullet} \rightarrow H_2O_2 \qquad 5 - 8 \times 10^9\,M^{-1}\,s^{-1} \tag{7}$$

$$2\,HO_2{}^{\bullet} \rightarrow H_2O_2 + O_2 \qquad 0.8 - 2.2 \times 10^6\,M^{-1}\,s^{-1} \tag{8}$$

$$HO^{\bullet} + HO_2{}^{\bullet} \rightarrow H_2O{+}O_2 \qquad 1.4 \times 10^{10}\,M^{-1}\,s^{-1} \tag{9}$$

Equations (1–5) are the rate limiting steps in the Fenton chemistry since H_2O_2 is consumed and Fe^{2+} is regenerated from Fe^{3+} through these reactions. Equations (6–9) are proposed also to occur in Fenton processes.

Besides Fe(II), other transition metal ions such as Fe(III), Cu(I) or Mn(II) can promote similar processes, which are then called Fenton-like or Fenton type. The efficiency is lower with Fe^{3+} than when using Fe^{2+} because of the lower reactivity of Fe^{3+} towards H_2O_2.

Regarding the fate of the generated $HO^{\bullet}$, this species can oxidize Fe^{2+}, eq. (3), but this will be an unproductive reaction regarding its utility for transformation of pollutants. Otherwise, $HO^{\bullet}$ are able to react by hydrogen abstraction from aliphatic carbon atoms, eq. (10), electrophilic addition to double bonds or aromatic rings, eq. (11), and electron transfer reactions, eq. (12). $HO^{\bullet}$ can also oxidize metals or metalloids such as As(III). The hydroperoxyl radicals, $HO_2{}^{\bullet}$, can react with organic compounds, but they are less sensitive than $HO^{\bullet}$.

$$RH + HO^{\bullet} + H_2O \rightarrow ROH + H_3O^+ \tag{10}$$

$$R - CH = CH_2 + HO^{\bullet} \rightarrow R - C^{\bullet}H - CH_2OH \tag{11}$$

$$RX + HO^{\bullet} \rightarrow RX^{\bullet +} + HO^- \tag{12}$$

Fe^{3+} and Fe^{2+} can oxidize or reduce organic radicals, or the radicals can recombine:

$$R^{\bullet} + Fe^{3+} \rightarrow R^+ + Fe^{2+} \tag{13}$$

$$R^{\bullet} + Fe^{2+} \rightarrow R^- + Fe^{3+} \tag{14}$$

$$2R^{\bullet} \rightarrow R - R \tag{15}$$

After the work of Walling [25], the radical mechanism has been broadly accepted for reactions in acid media, but the existence of the second mechanism [13, 21, 33, 34] was suggested from several evidences, e. g. molecular dynamics simulations of the Fe^{2+}/H_2O_2 system (33) and DFT studies [35], where it was proposed that the FeO^{2+} radical [36] is the transitory species instead of $HO^{\bullet}$. According to Kremer [30, 31], the mechanism of the Fenton reaction is based on the following steps:

$$Fe^{2+} + H_2O_2 \rightarrow \left\{Fe^{2+\bullet}H_2O_2\right\} \rightarrow FeO^{2+} + H_2O \tag{16}$$

$$FeO^{2+} + H_2O_2 \rightarrow Fe^{2+} + O_2 + H_2O \tag{17}$$

$$FeO^{2+} + H^+ + Fe^{2+} \rightarrow 2Fe^{3+} + 2HO^- \tag{18}$$

$$FeO^{2+} + Fe^{3+} \rightarrow \{FeOFe\}^{5+} \tag{19}$$

$$\{FeOFe\}^{5+} + H_2O_2 \rightarrow Fe^{2+} + Fe^{3+} + O_2 + H_2O \tag{20}$$

The intermediate ferryl ion (FeO^{2+}, involving Fe(IV)) oxidizes HA or H_2A species yielding Fe^{3+} or Fe^{2+}:

$$FeO^{2+} + HA \rightarrow A + Fe^{3+} + HO^- \tag{21}$$

$$FeO^{2+} + H_2A \rightarrow A + Fe^{2+} + H_2O \tag{22}$$

The formation of a hydroperoxy complex $[Fe(OOH)]^{2+}$ was also proposed as an intermediate in Fenton mechanisms at pH < 2 and at very high H_2O_2 concentrations in homogenous solution [37]:

$$Fe^{2+} + H_2O_2 \rightarrow [Fe\,(OOH)]^{2+} + H^+ \rightarrow FeO^- + HO^{\bullet} + H^+ \tag{23}$$

where Fe^{2+} is oxidized through an inner sphere electron transfer mechanism. Other complexes, formulated as $[Fe(OH)]^{2+}$ or $[Fe(OH)(HO_2)]^+$, can be found in Fenton reactions [37, 38], together with the peroxo complex ($Fe(OOH)^+$) [1].

Bossmann et al. [39] postulated the formation of an iron(IV) complex (Fe^{4+}(aq)), which may react further, leading to the formation of a free $HO^{\bullet}$ and Fe^{3+}(aq).

1.2.2 Advantages and disadvantages of the Fenton processes

The common Fenton process occurs at room temperature and atmospheric pressure. The reagents are easy to acquire, store and handle, and they do not represent an environmental problem. Nevertheless, the formation of a solid sludge due to the precipitation of iron oxides, and the wastage of H_2O_2 represent two important disadvantages in this treatment [6]. Due to the fact that the rate constant of eq. (1) is much higher than that of eq. (2), the consumption of Fe^{2+} is more rapid than their regeneration. A large amount of ferric hydroxide as a sludge is formed during the process, posing additional separation and disposal problems, especially in the treatment of large volumes of water.

Also, the need of using high Fe^{2+} concentrations (40–80 ppm) is an important disadvantage of the Fenton homogenous processes [40, 41].

1.2.3 Influence of the temperature

The efficiency of the Fenton process is not affected if the temperature is increased from 10 to 40 °C [19], but if the temperature overcomes 40 °C, the reaction mixture should be cooled down. An optimum temperature of 30 °C was reported for Fenton reactions [20].

1.2.4 Influence of pH

In the Fenton process, the degree of reaction between Fe^{2+} and H_2O_2 species is highly related to the solution pH [26]. As said above, the optimum working pH is around 3, regardless of the target substrate [19, 42–44]. At pH < 1, the reaction is limited to the oxidation of Fe^{2+} by H_2O_2. Also, at pH below 3, a reduced efficiency in the degradation of a substrate by the Fenton reaction was noticed [45]. This effect is in part caused by the formation of $[Fe(H_2O)_6]^{2+}$ complexes at low pH, which makes slower the reaction between Fe^{2+} and H_2O_2 [46]. Solvation of H_2O_2 in presence of H^+ to form $[H_3O_2]^+$ enhances the stability of H_2O_2 and reduces its reactivity with Fe^{2+} [45, 47]. Above pH 1 and in the presence of an excess of H_2O_2, the decomposition of H_2O_2 occurs:

$$2H_2O_2 \rightarrow O_2 + 2H_2O \tag{24}$$

The formation of relatively inactive iron oxohydroxides, precipitation of ferric hydroxide and the acceleration of the H_2O_2 autodecomposition are favored at high pH [48], reducing consequently the reactivity of the Fenton reagent. Due to the existence of less free iron ions, less $HO^\bullet$ are generated in the media; besides, the oxidation potential of this radical diminishes when the pH is increased [6, 49]. Thus, Fenton reactions for the degradation of several compounds are considerably reduced at low and high pH values as well.

1.2.5 The photoFenton process

Fenton (H_2O_2/Fe^{2+}) and Fenton-like (H_2O_2/Fe^{3+}) can be highly improved under UV/visible irradiation ($\lambda < 600$ nm). As opposed to dark Fenton processes, where Fe^{3+} ions are accumulated in the system and the reaction cannot proceed once Fe^{2+} ions are totally consumed, in the photoFenton reaction, Fe^{2+} ions are regenerated from Fe^{3+} by photoreduction. The enhancement was explained by four main reasons [50]:

1. Photolysis of iron (III) hydroxocomplexes ($\lambda < 580$ nm) yields extra $HO^\bullet$ and regenerates Fe(II) (eqs. (25) and (26)) by a metal to ligand charge transfer reaction [51–53]:

$$\left[Fe(OH)^{2+}\right] + h\nu \rightarrow Fe^{2+} + HO^\bullet \tag{25}$$

$$\left[Fe\,(H_2O)\right]^{3+} + h\nu \rightarrow Fe^{2+} + HO^\bullet + H^+ \tag{26}$$

1. Photogenerated Fe(II) participate in the Fenton reaction of eq. (1) to produce additional $HO^\bullet$, increasing the oxidation rate in comparison with the dark Fenton process [54, 55].

2. If $\lambda < 310$ nm is used, photolysis of H_2O_2 via irradiation at short wavelengths takes place [50]; the production of $HO^\bullet$ by direct photolysis is an additional $HO^\bullet$ source:

$$H_2O_2 + h\nu \rightarrow 2HO^\bullet \tag{27}$$

1. Photolysis of Fe(III) chelates (Fe_3L) formed between Fe^{3+} and the organic substrate, its degradation intermediates or other possible ligands present in the reaction medium, makes efficient the use of the photons up to the visible [1, 56]:

$$[Fe_3L] + h\nu \rightarrow [Fe^{3+}L]^* \rightarrow Fe^{2+} + L^\bullet \tag{28}$$

Depending on the ligand, the Fe(III) complexes can have different light absorption properties, and reactions of eqs. (25), (26) and (28) take place with different quantum yields and at different wavelengths. Fe(III)-carboxylate complexes have much higher quantum yields than Fe(III)-water complexes and promote the reaction intensively. However, the presence of iron complexes in the media can promote a lesser photodegradation of organic contaminants due to their stronger capacity to absorb radiation [57, 58].

In addition, the total amount of iron needed and the sludge generation processes are considerably reduced in the photoFenton system [59]. Consequently, this increases the degradation rate of organic pollutants, such as 4-chlorophenol (4-CP), nitrobenzene (NB), anisole, polychlorinated biphenyls (PCBs) and herbicides [51, 60, 62–64].

The best performance of the photoFenton process is also at pH around 3 because of the formation of Fe(III)-hydroxyl complexes from Fe^{3+} and water. At pH 2.8, the dominant iron species in solution is $[Fe(OH)]^{2+}$,

which is also the most photoactive Fe(III)-water complex. These complexes start to dissociate between pH 2–4 as shown in eqs. (29) and (30). These species are also more soluble, making less possible precipitation of iron [51, 65]:

$$\left[Fe(H_2O)_6\right]^{3+} \rightleftharpoons \left[Fe(H_2O)_5\,(HO)\right]^{2+} + H^+ \tag{29}$$

$$\left[Fe(H_2O)_5\,(HO)\right]^{2+} \rightleftharpoons \left[Fe(H_2O)_4(HO)_2\right]^{+} + H^+ \tag{30}$$

Thus, species such as $Fe(OH)^{2+}$ and $[Fe(H_2O)_5(HO)]^{2+}$ are more photoactive or photosensitive to electromagnetic radiation comprised in the 280–405 nm range; this allows the use of sunlight for reactions of eqs. (25) and (31):

$$\left[Fe\,(OH)\,(H_2O)_5\right]^{2+} + H_2O + h\nu \rightarrow \left[Fe(H_2O)_6\right]^{2+} + HO^{\bullet} \tag{31}$$

Pignatello and coworkers [21] suggested the participation in these systems not only of ferryl but also of Fe(V)=O species in conjunction with visible absorbing iron species.

Acid conditions around pH 3 also favor the conversion of the $HO^{\bullet}$ scavengers carbonate and bicarbonate into carbonic acid, which has a low reactivity against $HO^{\bullet}$ [66]. However, in photoFenton experiments in the presence of oxalate, citrate or in the absence of organic ligands, $HO^{\bullet}$ production rate was equal to Fe^{2+} photoproduction rate, revealing that, at pH 3–8, $HO^{\bullet}$ was generated with a perfect yield in the photoFenton reaction [63]. In the same way, formate oxidation rates were consistent with $HO^{\bullet}$ formation in the photoFenton reaction at pH 6 and in the presence of fulvic acid [67]. Otherwise, the study of photoFenton reactions in natural waters at circumneutral pH suggested that oxidant species such as $HO^{\bullet}$ and ferryl could be significant for contaminant degradation [54].

The photoFenton reactions are very useful to treat high strength organic wastewaters [54].

1.2.6 Heterogeneous Fenton reactions starting from zerovalent iron

As said, in the homogeneous Fenton processes, the use of Fe(II)/Fe(III) suffers from a major disadvantage, the need to remove a high amount of iron sludge after the water treatment. In addition, large amounts of Fe^{2+} are required (ca. 50–80 ppm), with a H_2O_2-Fe^{2+} molar ratio as high as 9:1. It is important to recall that it is mandatory to acidify the effluents before the reaction and subsequently neutralize the treated solutions before disposal. Due to these problems, in the mid-1990s, researchers started to develop heterogeneous catalysts for the Fenton reaction using solid iron-containing compounds or solid materials rich in iron for the degradation of a wide range of organics at lower operational cost [18, 40, 68–74]. Decomposition of aqueous H_2O_2 over some metals (Ag, Cu, Fe, Mn, Ni, and Pt) and their oxides on supported silica, alumina, and zeolites has been a subject of research since the beginning of the previous century [75]. In recent years, heterogeneous catalysts for the Fenton reaction have been increasingly developed. Clays, activated carbon, activated carbon impregnated with iron and copper oxide, metals, silicas, zeolites, iron or copper supported on zeolites, alumina, carbon and fly ashes catalysts, transition metal-exchanged zeolites, pillared clays, iron-oxide minerals, iron oxide nanocatalysts, metal-exchanged zeolites, hydrotalcite-like compounds, metal-exchanged clays, metal-exchanged resins and layered materials, Nafion film or Nafion, resin-supported Fe(II) or Fe (III), iron-containing ashes, iron-coated pumice particles, iron immobilized aluminates, etc., have been tested (see [70, 74] and references therein). Zerovalent state metals, such as Fe^0, Zn^0, Sn^0 and Al^0, are well known since several years ago for their effectiveness in remediation of contaminated groundwater [76, 77]. Also, iron oxides have been amply used.

Solid catalysts must satisfy a number of requirements for the use as Fenton reagents, as having high activity for contaminant removal, presenting no leaching of active cations, pH and temperature stability, and ability to promote a high H_2O_2 conversion with minimum decomposition. Also they should be reasonably priced. One of the most important advantages of the use of a heterogeneous catalyst is the possibility of its separation from the waste stream.

The use of zerovalent iron (ZVI) in a Fenton-type process for the degradation of pollutants (known as Advanced Fenton Process (AFP)) has become of considerable interest over the last few years as a way to avoid or at least reduce the problems arising in homogeneous Fenton processes. It can be proposed that oxidation occurs through two different mechanisms: a) from iron ions released into solution, or b) through reactions between solutes and surface-species. The use of these materials avoids the precipitation of iron hydroxides/oxides because few iron ions are present in the aqueous phase, with the easy separation of the catalyst after the application (and

possible reuse in some cases), and the broadening of the pH working range as additional advantages. Although different types of ZVI have been used in Fenton processes, and many papers have been published, we will only focus in this review on the use of ZVI materials in combination with H_2O_2 due to the higher performance in remediation reactions.

An important disadvantage of heterogeneous reactions is that target molecules must diffuse to the surface of the material to reach active sites before their degradation. Also, these reactions are generally much slower than the homogeneous ones at the same concentrations; however, heterogeneous reactions are sometimes more efficient as they consume less H_2O_2.

1.2.7 Mechanism of heterogeneous Fenton and photoFenton reactions with zerovalent iron

Using iron particles together with H_2O_2, reactions additional to (1–23), dealing with iron corrosion, have to be considered [78]. ZVI undergoes a series of corrosion reactions in water. The anodic process is the dissolution of Fe(0), while the cathodic process is the evolution of H_2(g) under anaerobic conditions and O_2 reduction under oxic conditions [79, 80]. Metallic iron (Fe(0)) produces, upon immersion, iron corrosion products including nascent oxides and Fe^{2+}, which play a crucial role in H_2O_2 activation.

A simplified scheme of the mechanism for Fenton reactions with zerovalent iron is shown in Figure 1.

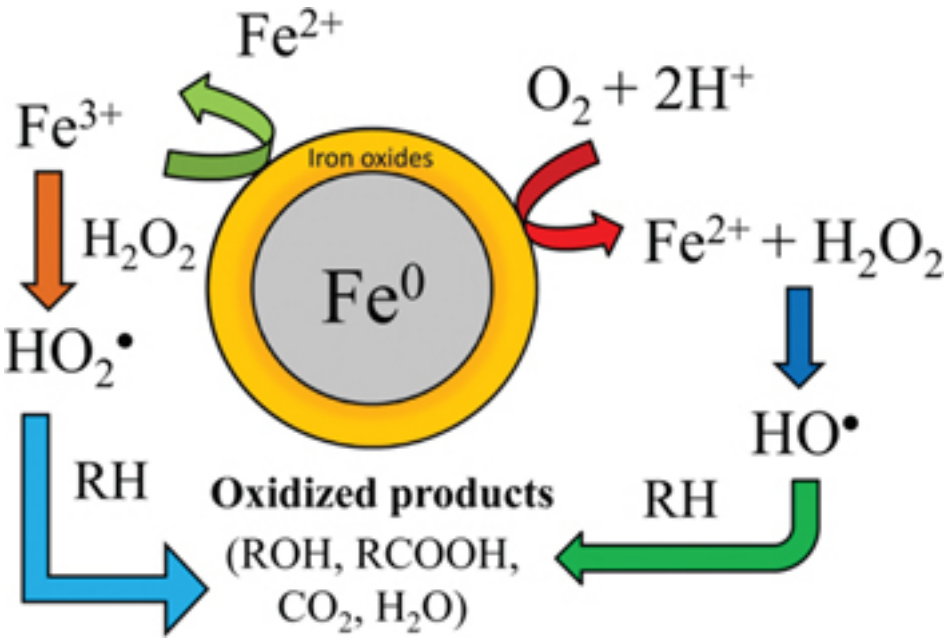

Figure 1: Simplified mechanism of heterogeneous Fenton reactions with ZVI.

According to Figure 1, Fe^0 is oxidized by O_2 producing Fe^{2+} and H_2O_2. In addition, Fe^0 can reduce Fe^{3+} to Fe^{2+}. Then, the course of reactions would follow the Fenton typical mechanisms to yield oxidized products or the total mineralization of the organic compound.

A detailed mechanism involves the following processes. Oxidation of Fe(0) by H^+ in the absence of O_2 yields Fe^{2+} (eq. (32)), which is available for reaction with H_2O_2 (eq. (1)). Equation (33) is the reaction of ZVI with H_2O_2, ending in water production. Degradation and oxidation of organic compounds by $HO^\bullet$ take place through eqs. (10–13).

$$Fe(0) + 2H^+ \rightarrow Fe^{2+} + H_2 \tag{32}$$

$$Fe\,(0) + H_2O_2 + 2H^+ \rightarrow Fe^{2+} + 2H_2O \tag{33}$$

In the presence of oxygen, the following additional equations take place.

$$Fe(0) + O_2 + 2H^+ \rightarrow Fe^{2+} + H_2O_2 \tag{34}$$

$$2Fe\,(0) + O_2 + 4H^+ \rightarrow 2Fe^{2+} + 2H_2O \tag{35}$$

$$2Fe(0) + O_2 + 2H_2O \rightarrow 2Fe^{2+} + 4HO^- \quad (36)$$

$$6Fe^{2+} + O_2 + 6H_2O \rightarrow 2Fe_3O_4 \downarrow + 12H^+ \quad (37)$$

$$4Fe^{2+} + O_2 + 10H_2O \rightarrow 4Fe(OH)_3 \downarrow + 8H^+ \quad (38)$$

$$4Fe^{2+} + O_2 + 6H_2O \rightarrow 4FeOOH \downarrow + 8H^+ \quad (39)$$

In addition, faster recycling of Fe^{3+} at the iron surface takes place through the following reaction [81]:

$$2Fe^{3+} + Fe\,(0) \rightarrow 3Fe^{2+} \quad (40)$$

Of course, once Fe^{2+} is formed, reaction of eq. (1) begins to be operative, and the $HO^{\bullet}$ contributes to the oxidizing capability of the system [82]. Therefore, reactive oxygen substances (ROS) including H_2O_2 and $HO^{\bullet}$ are generated in the $Fe(0)/H_2O/O_2$ system under acidic conditions through the two-electron oxidation of Fe(0) followed by the Fenton reaction (eqs. (1) and (34)). In the pH range of natural waters, Fe^{2+} may hydrolyze and form $Fe(OH)_2$ at the Fe(0) surface (eq. (42)). Fe^{2+} is very sensitive to O_2, and its oxidation by O_2 is quite rapid, increasing the reaction rate with pH. The resulting Fe^{3+} readily hydrolyzes, precipitates and transforms to (hydr)oxides such as Fe_3O_4, $Fe(OH)_3$, FeOOH (eqs. (37–39), depending on the O_2 availability, forming a thick layer of iron oxides, even more oxidized like maghemite or lepidocrocite, thereby decreasing the reactivity of ZVI.

The kinetics of iron corrosion depends on the intrinsic reactivity of the used Fe(0) material and other factors such as O_2 concentration and pH. The corrosion rate decreases with increasing pH up to pH 4, becomes almost stable at pH between 4 and 10 and decreases slightly above pH 10. Fe^{2+} recycling also occurs in the presence of Fe^{3+} (eq. (40), but this phenomenon is not favored, since the solubility of Fe^{3+} is very limited at pH > 5.

$$Fe(0) + 2Fe^{3+} \rightarrow 3Fe^{2+} \quad (41)$$

$$Fe^{2+} + 2H_2O \rightarrow Fe(OH)_2 \downarrow + 2H^+ \quad (42)$$

Instead, Fe^{2+} can be regenerated after reaction of radical species with Fe^{3+} (eq. (13) [83].

The mechanisms of oxidation in the ZVI/O_2 system are pH dependent. Under acid conditions, oxidation takes place by H_2O_2 generated during ZVI oxidation, which then reacts with Fe^{2+} via the Fenton reaction (eq. (1)) to produce $HO^{\bullet}$ [84, 85]. At neutral pH values, Fe^{2+} oxidation by O_2 produces a different oxidant, most likely the ferryl ion (Fe(IV)) (eq. (16) [2, 84, 85].

An excess of ZVI can be detrimental, as it can promote the decomposition of H_2O_2 toward non-reactive oxygen species (eq. (33)), and the scavenging of $HO^{\bullet}$ (eq. (1)) [83]. Iron metal sheets showed to be corroded in the presence of phenol and benzoic acid together with H_2O_2. Iron corrosion increased with the decrease of pH (in the range 1.5–3.0) [86, 87].

1.2.8 Examples of heterogeneous Fenton reactions using macro- or microsized zerovalent iron materials

Initially, microsized iron, e. g., iron powders at different sizes (from a few to hundreds of microns) has been used. For example, Wada et al., possibly the first study of a Fenton reaction using metallic iron, examined the oxidation of components of a wastewater using H_2O_2 and iron powder [88]. The initial wastewater had a chemical oxygen demand (COD) of 4500 mg L^{-1}. This COD was decreased up to 160 mg L^{-1}, while using ferrous sulfate in solution, COD was reduced only to 270 mg L^{-1}. Additionally, the amount of Fe-ions in solution coming from the iron powder was less than half of that from $FeSO_4$, leading to a reduced volume of sludge. The authors proposed that a heterogeneous mechanism participated in the H_2O_2 decomposition.

Takemura et al. [89] investigated steel wool, steel foil, and reticulated iron (manufactured by impregnating urethane foam with an iron powder slurry) to oxidize perchloroethylene (PCE) in the presence of H_2O_2. All solids reduced the PCE concentration from 100 mg L^{-1} to less than 0.1 mg L^{-1} in 24 h, but the reaction with reticulated iron could be conducted at pH 5–9 with no apparent iron oxide byproduct. While organic chlorine compounds added in pure water were easily decomposed by the Fenton reaction using reticulated iron, it was difficult to achieve high efficiency in the case of a real wastewater from a laundry process. This effect was explained by the coexistence of competing high COD residuals, such as dirt and organic acids.

Tang and Chen [68] studied the oxidation of three dyes, Reactive Red 120, Direct Blue 160, and Acid Blue 40, by the use of iron powder (<10 µm size) and H_2O_2, finding the optimal pH between 2 and 3, depending on the structure of the dyes and the dissolution rate of iron. The authors concluded that the combination H_2O_2/Fe powder was better than the homogeneous Fenton process due to the continuous dissolution of iron and the possibility of adsorption of the dye on the iron powder. The authors proposed that, at pH below 2.5, dye removal occurred mainly by adsorption, whereas, at higher pH values, where adsorption was less important, addition of H_2O_2 doubled (at pH 3) or quintupled (at pH 3.5) dye removal to more than 90 % of the initial concentration.

Lücking et al. [90] reported the use of iron powder (70–100 µm) to replace iron salts as a catalyst for Fenton reactions, and tested the system in the oxidation of 4-CP with H_2O_2. Using iron powder (1 g L^{-1}) and 5.3 g L^{-1} H_2O_2, a stoichiometric production of Cl^- and 50 % DOC removal after 2 h were obtained for 1 g L^{-1} 4-CP. In contrast, the Fenton reaction (1 mg L^{-1} Fe^{2+}, added as $FeSO_4$), gave only 40 % Cl^- production and 5 % DOC removal after 150 h. Later, the same system was studied by Zhou et al. [91]. At an initial pH of 4, the degradation kinetics of 4-CP followed a two-stage first-order: an initial slow degradation stage followed by a rapid second degradation stage, with a kinetic constant one magnitude larger than that of the former stage. A scheme of 4-CP degradation pathways in the system was proposed, where the molecule is attacked by HO• forming *p*-chlorophenolperoxyl radicals, finally leading to the production of low molecule aliphatic organic acids (Figure 2).

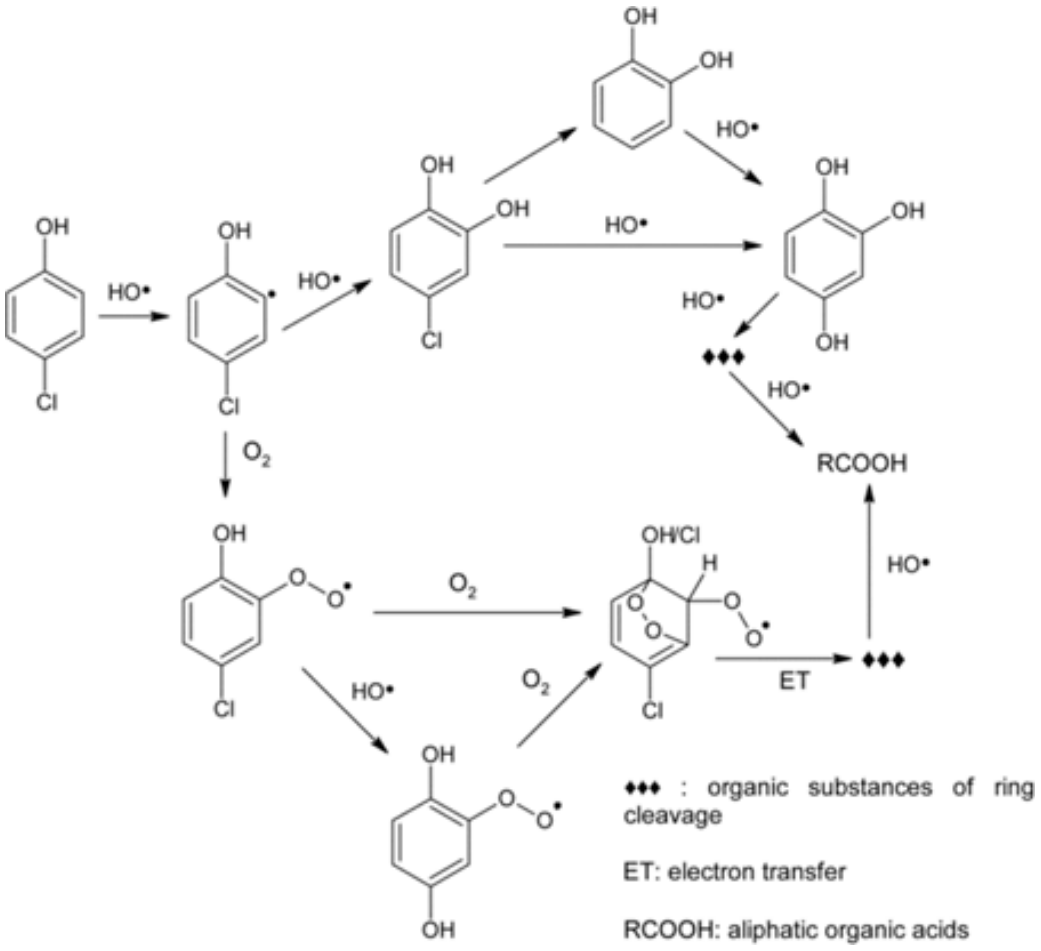

Figure 2: Degradation pathways of 4-CP with the nZVI/H_2O_2 system (adapted from reference [91]).

Bremner et al. [81] studied the degradation of phenol (1 g L^{-1}) with ZVI (iron bars, 80 × 25 × 1 mm, cut from an iron sheet (99.5 % pure)) and relatively concentrated H_2O_2 (9.5 M) in 1 M H_2SO_4. The degradation of phenol and of its degradation intermediates (catechol, hydroquinone, benzoquinone and maleic acid) was complete after 15 min of reaction, although an unknown compound (suspected to be an organic complex of iron and catechol) began to appear. The reaction a pH 6 was slower, with the complete phenol degradation after 2 h, but about 4 h were needed for the disappearance of most of the intermediates. Under less stringent conditions (6 mL of 0.34 M H_2O_2) in the absence of acid, the same products were obtained but formed over a much longer timescale, with only a partial removal of phenol (40 %) after 10 h.

Kallel et al. [92] pretreated an olive mill wastewater (OMW, COD 19 g L^{-1}, pH 5.2) with ZVI (a residual product from a metal turner) and H_2O_2 to improve the degradation of phenolic compounds and COD removal.

The optimal conditions (92 % COD removal in 1 h) were the continuous presence of iron metal, pH 2–4 and 1 M H_2O_2. The biodegradability of the OMW increased during the treatment. In a further work [93], a conventional Fenton process (CFP) was compared with an AFP (using iron particles of 10 µm size) for the removal of COD and phenol from an OMW. It was observed that COD and phenol were removed by AFP more rapidly compared with the CFP [93]. The optimum conditions for CFP were $[Fe^{2+}] = 1500$ mg L^{-1}, $[H_2O_2] = 1750$ mg L^{-1}, pH 4.6 (original pH of the OMW), which yielded 82.4 % COD and 62 % removal of phenolic compounds. For AFP, the optimum conditions were [Fe(0)] = 2000 mg L^{-1}, $[H_2O_2] = 2000$ mg L^{-1}, pH 3, with 82 % COD and 63.4 % removal of phenols. Even though COD and phenol removal efficiencies were very close, COD and phenol removal rates of AFP were higher than those of CFP.

A degradation system using commercial iron wool as iron source and H_2O_2 was employed for the degradation of diuron in a flow system where the solution passed through the iron wool. The pH and H_2O_2 concentration were varied from 2.5 to 8.5 and from 2 to 4 M, respectively; Fe amount was evaluated from 1 to 3 g in the best pH and H_2O_2 concentration. In the best condition (pH 2.5, 2 g of iron, and 2 mM of H_2O_2), diuron (10 mg L^{-1}) was completely removed from the solution in 10 min of reaction [94]. The process also resulted in an excellent degree of effluent mineralization, with *ca*. 40 % TOC removal in 10 min of treatment.

The pretreatment of a pharmaceutical wastewater by Fenton oxidation with ZVI and H_2O_2 was investigated by Segura et al. [83] to improve the degradation of the mixture of organic compounds present in the wastewater. Commercial iron metal powder and iron shavings obtained from wastes from a metallurgical process were used. The optimal conditions for degradation led to TOC reductions of up to 80 % in only 1 h of treatment. Moderate loadings of ZVI and H_2O_2 (ZVI/TOC weight and H_2O_2/TOC molar ratios of 12 and 3.2, respectively) were used. As said before and found by the authors, an excess of ZVI was detrimental due to H_2O_2 decomposition toward non-reactive oxygen species and $HO^{\bullet}$ scavenging (eqs. (1) and (33)).

Fu et al. [95] reported the degradation of the Acid Red 73 (AR 73) azo dye by a Fenton process using ZVI (analytical grade, 99 % purity, 200 mesh) and H_2O_2. Various amounts of ZVI and H_2O_2 were tested (solid/liquid ratios of 0, 0.1, 0.2, 0.3 and 0.4 g L^{-1}) or H_2O_2 concentration of 0, 1.0, 2.0, 2.5 and 3.0 mM. The pH was varied from 2 to 5. AR 73 removal efficiency (measured by absorbance at 509 nm) increased with the increase of the ZVI amount, H_2O_2 concentration, mixing rate and temperature, but decreased with the increase of pH. After 30 min of reaction time, the color removal percentage was 97.0, 96.8 and 89.8 % at initial dye concentrations of 100.0, 200.0 and 300.0 mg L^{-1}, respectively. At the optimum conditions, [ZVI] = 0.3 g L^{-1}, $[H_2O_2] = 2.0$ mM, mixing rate = 100 rpm, $T = 20$ °C, pH 3, the residual AR 73 concentration ($[AR\ 73]_0 = 200.0$ mg L^{-1}) could be reduced to only 6.4 mg L^{-1} after 30 min treatment.

The treatment of a coking wastewater was investigated by an AFP using Fe powder (30–70 µm, purity higher than 98 %) and H_2O_2 [96]. Higher COD and higher total phenol removal rates were achieved with a decrease in the initial pH and an increase in H_2O_2 dosage. At pH < 6.5 and $[H_2O_2] = 0.3$ M, COD removal reached 44–50 %, and approximately 95 % of total phenol was removed after 1 h. The oxygen uptake of the effluent at 1 h increased ca. 65 % compared with that of the raw coking wastewater, indicating a significant improvement of the biodegradation. Various organic compounds present in the wastewater, such as bifuran, quinoline, resorcinol and benzofuranol, were removed completely.

Two papers reported the treatment of soils using ZVI and H_2O_2. In the first one [97], a TNT-contaminated soil was treated by AFP, CFP, and calcium peroxide. All the treatments reduced TNT soil concentration below the required USEPA goal (17.2 mg TNT kg^{-1}). Using 2 % (w/w) fine-grained Fe(0) with a surface area of 3.3 m^2 kg^{-1}, TNT soil concentration in the treated soil at pilot scale (5 mg kg^{-1}) was reduced below the required standard within 4 h; however, in this case, no significant TNT destruction improvement was observed when 2 % Fe(0) (w/w soil) was combined with four sequential additions of 0.25 % H_2O_2. In contrast, a time greater than 24 h was required either with the aqueous Fenton reagent (Fe^{2+}/H_2O_2) or with CaO_2. In the second paper [98], nanoscale zerovalent iron was used and it will be described in the following section.

Another strategy involves the sequential use of ZVI and CFP and was observed in three papers. Barreto-Rodrigues et al. [99] explored the use of commercial iron wool combined with Fenton processes for the treatment of a wastewater of the 2,4,6-trinitrotoluene (TNT) industry. The wastewater had pH 1, COD = 638 mg L^{-1} and [TNT] = 156 mg L^{-1}, and various treatability experiments were conducted at different pH values (1.6, 3.0, 5.0, 7.0 and 8.3), amounts of metallic iron (0, 0.2, 0.6, 1.0 and 1.3 g) and reaction times (0, 6, 15, 24 and 30 min) according to an experimental design using a response surface methodology. The optimization study indicated that the acid pH favored the leaching of the iron wool, and the most efficient condition, which produced an 80 % TNT conversion, was at pH 3 and with an iron wool mass of approximately 3.2 g L^{-1}. This condition supplied sufficient amounts of Fe(II) in solution for an oxidative treatment through the Fenton reaction. The residual Fe(II) was used with the addition of H_2O_2 (30 %) at a Fe^{2+}:H_2O_2 ratio of 1:5 to complete the treatment. The process was highly efficient since it reduced acute toxicity, removed 100 % of TNT, 100 % of the organic nitrogen and 95.4 % of the COD. The main advantage was associated with the primary conversion of TNT in chemical species with a greater susceptibility to oxidative degradation. It is important to point out that the Fenton or

photoFenton processes using Fe^{2+} did not significantly remove TNT, total nitrogen or COD, strengthening the hypothesis that the treatment with the iron wool forms chemical species with increased biodegradability, more easily degraded by the Fenton process.

In another work [100], NB was treated submitting first the pollutant to a ZVI pretreatment to avoid direct oxidation through the CFP, which produces a considerable amount of highly toxic 1,3-dinitrobenzene (1,3-DNB) as byproduct. Both, ZVI treatment and CFP were first optimized independently and then, the ZVI-Fenton integrated system (Figure 3) was constructed and tested to degrade NB. Since the ZVI pretreatment could produce a sufficient amount of ferrous ions for the subsequent Fenton oxidation, the addition of Fe^{2+} to the Fenton reactor in the integrated system was not required. Aniline and ferrous irons were generated in the ZVI pretreatment, and it was proved that they produced an inhibitory effect on the formation of 1,3-DNB in the Fenton process. For the integrated process, ZVI was added into the wastewater at 1.5 kg m^{-3} at pH in the 1.8–2.2 range, and H_2O_2 aqueous solution was added at 40 kg m^{-3}. The integrated system achieved a high NB removal efficiency (93.0 %), producing only 0.4 % 1,3-DNB. The integrated system increased the biodegradability and decreased the acute toxicity of the wastewater significantly more than the CFP. A NB-rich (1.15 mM) wastewater from a chemical plant was treated by the novel ZVI-Fenton integrated system. For the ZVI pretreatment, ZVI was added at 1.5 kg m^{-3} at pH 2. For the subsequent Fenton oxidation, 10 kg m^{-3} H_2O_2 (27.8 %, w/w) was added at pH 3, and no ferrous sulfate was necessary. The novel ZVI-Fenton integrated process achieved 96.2 % NB removal, with a low content of DNB isomers (0.8 mg L^{-1}), showing an increase in the biodegradability and a reduction in the acute toxicity in comparison with the untreated wastewater with a relatively low operation cost.

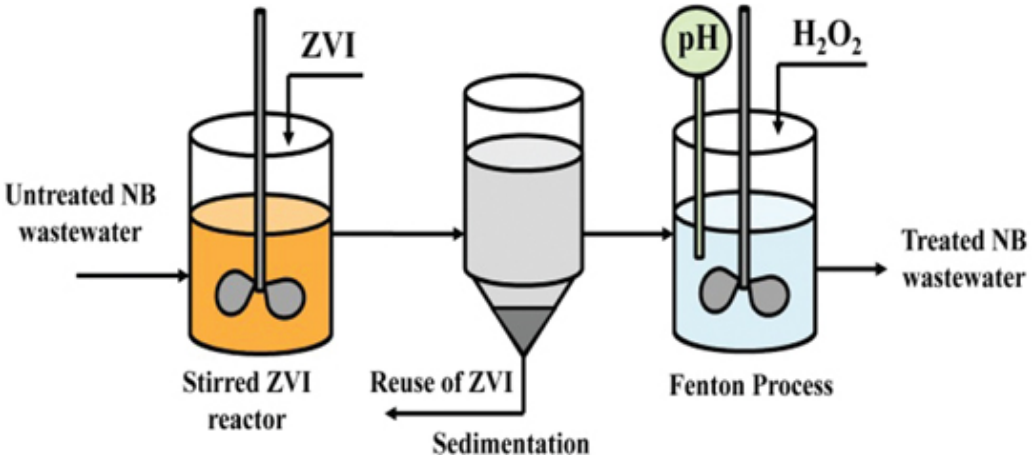

Figure 3: Integrated ZVI-Fenton system for NB treatment (adapted from reference [100]).

In a third paper, ZVI (2.0 g L^{-1}) was used to pretreat *p*-chloronitrobenzene (*p*-CNB, 25 mg L^{-1}, pH 3). *p*-CNB could be completely transformed in 3 h, and the major product was *p*-chloroaniline (*p*-CAN). Adding H_2O_2 to the system after reaction, further *p*-CAN degradation was obtained, attributed to Fenton oxidation due to Fe^{2+} released (50.4 mg L^{-1}) during the ZVI corrosion. The sequential treatment was more effective than a Fenton oxidation alone since the removal rate of total organic carbon (TOC) was improved by about 34 %. It was suggested that the amino function group of *p*-CAN is more susceptible to oxidative radical attack than the nitro function group of *p*-CNB [101].

A combination of ZVI reduction, Fenton oxidation process and biological treatment was tested for a wastewater containing 2,4-dinitroanisole (DNAN, 123.1 mg L^{-1}), 2,4-dinitrochlorobenzene (DNCB, 249.3 mg L^{-1}) and 2,4-dinitrophenol (DNP, 110.4 mg L^{-1}) at pH 7.2. Iron scrap, especially 30CrMoSi steel shavings containing more than 95 % iron, was used for the ZVI process. When ZVI was used alone (with iron shavings modified with 0.2 wt.% of copper on the iron surface by reductive precipitation), almost complete reduction of all nitroaromatic compounds was achieved at an empty bed contact time (EBCT) of 8 h, with removal efficiencies of 99.8, 99.9 and 97.9 % for DNAN, DNCB and DNP, respectively. The effluent of the ZVI bed was further treated in a column shaped Fenton reactor with H_2O_2 and $FeSO_4 \cdot 7H_2O$ solutions; the optimal pH, H_2O_2 to Fe(II) molar ratio, H_2O_2 dosage and hydraulic retention time were found to be 3, 15, 0.216 mol L^{-1} and 5 h, respectively. By the pretreatment by the combined ZVI-Fenton process under the optimal conditions, the aromatic organic compound removal achieved 77.2 %, while the majority of COD remained. The effluent of the Fenton reactor entered a coagulation-sedimentation tank containing 1 M Na_2CO_3 (pH 7.5–8.0), for precipitation of Fe(II) and Fe(III) ions and coprecipitation of byproducts. The sludge was separated through a sedimentation tank, and the supernatant was submitted to an anaerobic/aerobic biotreatment. Figure 4 shows the integrated system at bench scale. Then, a coupled ZVI-Fenton-biological process was operated for 3 months. Although COD and

TOC removal were not high (54.0 and 39.5 %, respectively), the ZVI-Fenton coupled process exhibited an excellent performance on removal of aromatic compounds, toxicity and color reduction. The reduction of biological toxicity reflected the improvement of biodegradability [102].

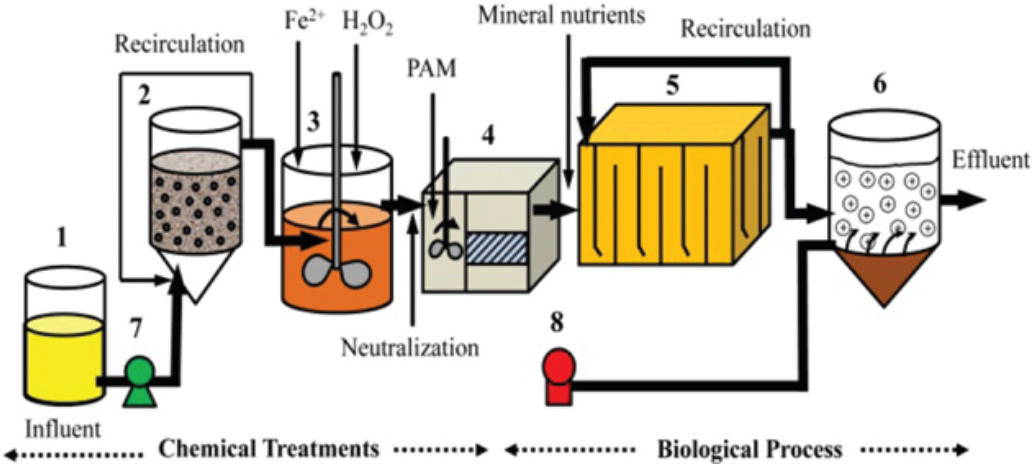

Figure 4: Bench scale experiment for the integrated ZVI-Fenton-biological treatment: (1) reservoir; (2) ZVI bed; (3) Fenton reactor; (4) coagulation-sedimentation tank; (5) anaerobic reactor; (6) biofilm reactor; (7) peristaltic pump; (8) air pump (adapted from reference [102]).

1.3 Zerovalent nanoparticles (nZVI)

1.3.1 A brief description of the characteristics of nZVI

In recent years, several works reported the use of nanoparticulate zerovalent iron (nZVI) in Fenton reactions. Nanoparticles possess inherent characteristics, quite different from those of the macroscopic or bulk iron forms, which makes them to present highly improved catalytic properties. The activity and selectivity of nanocatalysts for removal of pollutants are strongly dependent on their size, shape, and surface structure, as well as on their bulk composition [103, 104].

Reducing the particle size of granular Fe(0) materials (mm) to 10–100 nm increases the surface area and thus the chemical reactivity. The higher efficiency of nano-Fe(0) for contaminant removal contrasted with the results using granular Fe(0) and is highly related to the surface to diameter ratio of the particles: the smaller the nZVI particle size, the larger the specific surface [105].

nZVI particles exhibit a typical core-shell structure. The core consists primarily of zerovalent iron whereas an oxide shell, composed of Fe(II) and Fe(III), is formed as a result of the oxidation of the metallic iron [103]. Some images about nZVI particles are shown in Figure 5 [106]. On the other hand, ZVI nanoparticles tend to quickly aggregate into micro- to millimeter scale flocs, because of magnetic attraction, the huge area to volume ratio, the high surface energy and the reactivity.

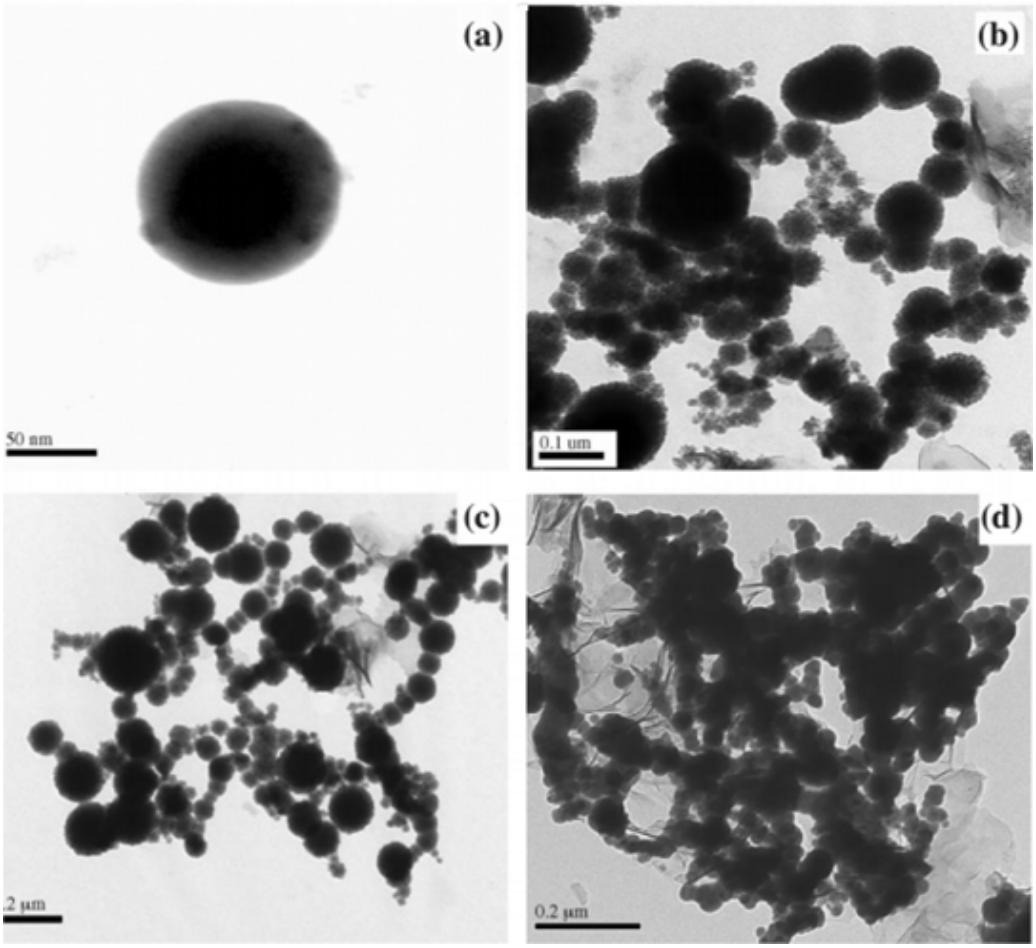

Figure 5. Micrographs of (a) a single nanoparticle, (b)–(d) aggregates of iron particles. From reference [106], with permission.

It has been reported that the use of nanoscale ZVI for remediation provides various advantages compared with microscale ZVI, including a decrease of the dosage, an increase of the rate, less risk of release of toxic intermediates, and generation of nontoxic final products [107].

1.3.2 Methods for synthesizing nZVI

Traditional methods to prepare nZVI particles are the bottom-up synthesis using aqueous-phase borohydride reduction [108–110], sonication and sol-gel methods [111, 112] and micro-emulsion-based techniques [113]. From them, the most widely used method was the borohydride reduction, as it uses less environmentally dangerous solvents or chemicals. The synthesis comprises the reduction of ferrous or ferric ions in aqueous solutions using sodium borohydride, a strong reducing agent, under inert conditions [110]:

$$2\mathrm{Fe}(\mathrm{H_2O})_6^{3+} + 6\mathrm{BH_4}^- + 6\mathrm{H_2O} \rightarrow 2\mathrm{Fe}^0\,(\mathrm{s}) + 6\mathrm{B(OH)_3} + 21\mathrm{H_2}\,(\mathrm{g}) \tag{43}$$

$$2\mathrm{Fe}^{2+} + \mathrm{BH_4}^- + 4\mathrm{H_2O} \rightarrow 2\mathrm{Fe}^0\,(\mathrm{s}) + \mathrm{B(OH)_4}^- + 4\mathrm{H}^+ + 2\mathrm{H_2}\,(\mathrm{g}) \tag{44}$$

However, the high cost of $NaBH_4$ is the major concern for the wet chemical synthesis of nZVI. On the other hand, amorphous iron nanoparticles (approximately 10 nm) can be fabricated by sonication of iron pentacarbonyl under Ar, yielding amounts of iron higher than 96 % [111, 114, 115]. Also, chemical vapor deposition (CVD) has been employed to synthesize iron nanoparticles [116]. Generally, the industrial nZVI is produced by thermal reduction of iron oxide precursors with hydrogen gas.

The top-down approach is the process of breaking large bulk materials to smaller particles, generally by mechanical means as ball milling [117]. Figure 6 shows SEM images of the microZVI precursor used in the ball milling process, and the final nanoscale material.

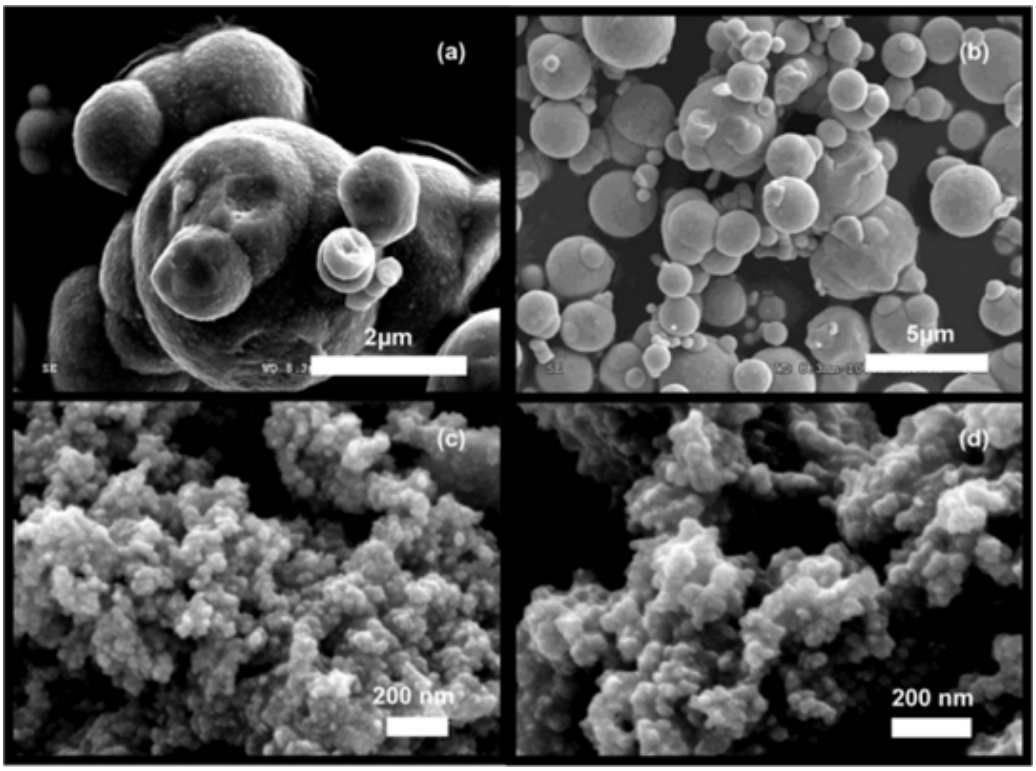

Figure 6: (a) and (b) SEM images of microiron (1–5 µm); (c) and (d) nanoiron (10–50 nm). From reference [117], reproduced by permission of The Royal Society of Chemistry.

A low-cost and green method for the synthesis of nanoparticles has been recently tested, which uses iron salts and polyphenolic compounds extracted from natural products (leaves or grains of plants), as tea leaves [118] or sorghum bran [119]. The concentration and type of the extracts has a high influence of size and morphology of the resulting nanoparticles. In this way, nZVI might be formed *in situ* by injecting the reductants into the subsurface to treat waters containing dissolved Fe^{2+}/Fe^{3+} ions. However, a discrepancy still exists on the composition and chemical structure of materials regarding if these nanoparticles are composed of Fe(0) or of iron oxides.

1.3.3 Examples of heterogeneous Fenton reactions using zerovalent iron nanoparticles

The mechanism of the heterogeneous Fenton process in the presence of nZVI has been proposed to be the same as that for macrosized iron (eqs. (32–40) plus (16) and (1)) [120, 121]. Actually, experiments performed by Xu and Wang with $HO^{\bullet}$ scavengers, such as n-butanol and KI, determined that these radicals, especially the surface-bounded $HO^{\bullet}$, had a dominant role in the degradation of organic compounds by AFPs using nZVI in the presence of H_2O_2 [122]. However, some degradation of the compounds was attributed to the action of alternative Fe(IV) species [36, 84, 85].

Bergendahl and Thies [123] investigated the use of nZVI, synthesized by reduction of $FeSO_4$ with sodium borohydride, for methyl tert-butyl ether (MTBE) oxidation. The conditions were: [MTBE] = 1000 mg L^{-1}, [nZVI] = 250 mg L^{-1}, a H_2O_2:MTBE molar ratio of 220 to 1 and pH 4. These conditions yielded over 99 % of MTBE degradation in 10 min, with significant generation (and subsequent degradation) of acetone as oxidation byproduct. At pH 7, MTBE was reduced in a similar extent (96 %) but, at pH 3, only 72 % of reduction efficiency was found. The rate of degradation of MTBE increased with the increase in the H_2O_2:MTBE ratio. Xu and Wang [122] reported the use of nZVI spheres (80–150 nm), prepared from KBH_4, for removal of 4-chloro-3-methylphenol (CMP) in the presence of H_2O_2. However, in this case, the CFP was much faster. The optimal dosage of reagents at pH 6.1 and [CMP] = 0.7 mM was 0.5 g nZVI L^{-1} and 3.0 mM H_2O_2. The increase of H_2O_2 concentration from 0.6 to 3.0 mM led to a gradual increase of the reaction rate; however, a further increase (up to 6.0 mM) was detrimental. This can be explained by $HO^{\bullet}$ scavenging by hydrogen peroxide, forming the less-reactive $HOO^{\bullet}$ species (eq. (44)).

$$HO^{\bullet} + H_2O_2 \rightarrow HOO^{\bullet} + H_2O \tag{45}$$

As mentioned before, Xu and Wang performed quenching experiments, with n-butanol and, especially iodide ions as surface radical quenchers, and proved that $HO^{\bullet}$ radicals, mainly surface-bonded $HO^{\bullet}$, were the main oxidants. However, as some degradation was still reached when n-butanol was added, it was suggested that some minor CMP degradation was due to alternative Fe(IV) species. Carboxylic acids and chloride ion were identified as degradation intermediates. Lepidocrocite (γ-FeOOH) was also detected, indicating that the initial nZVI is not stable and is transformed, impeding the reusability of the nanoparticles, a general detrimental characteristics of the material.

The performance of nZVI (prepared by reduction of $FeSO_4.7H_2O$ by $NaBH_4$) in the heterogeneous Fenton process was compared with electroFenton (EF), and photoelectroFenton (PEF) processes. Phenol was chosen as the model compound for degradation. The removal efficiency increased with an increase in nZVI dosage and decreased with an increase of the initial phenol concentration and initial pH. In one experiment with [phenol] = 200 mg L^{-1} at pH 6.2, the optimum dosage of nZVI and H_2O_2 for PEF was 0.5 g L^{-1} and 500 mg L^{-1}, respectively. The most efficient process was PEF, with a complete phenol removal in 30 min , compared with 65.7 and 87.38 % of phenol removal after 60 min for the Fenton and EF processes, respectively [120].

As said above [98], a paper reports the use of nZVI with H_2O_2 for treating soils. In this case, different sampled soils were contaminated with 1000 mg pentachlorophenol/kg and treated with different percentages of nZVI (synthetized from $NaBH_4$), and 1 % H_2O_2. Among three types of soils, the most effective was that with the highest content of ferrooxygen mineral, which helps to initiate the oxidation.

1.4 Advanced Fenton processes using modified iron particles and mixtures with iron oxides

Some successful results have been obtained in AFP using iron particles modified with metals or their mixtures with iron oxides, and they will be summarized below.

Composites with several Fe(0)/Fe_3O_4 ratios, prepared by two different methods, i) mechanical alloying of Fe(0) and Fe_3O_4 powders and ii) controlled (temperature-programmed) reduction of Fe_3O_4 with H_2, were prepared and tested in the methylene blue oxidation (MB) at different MB, iron promoter and H_2O_2 concentrations, and pH values [124, 125]. Conversion electron Mössbauer spectroscopy of a Fe(0)(50 wt%)/Fe_3O_4 composite indicated the lack of the Fe(0) signal, suggesting that the Fe(0) particles were located in the most internal part of the mixture and covered by the particles of the oxides; high resolution transmission electron microscopy studies showed that most of the small Fe(0) particles were surrounded by the oxide phase, indicating the existence of an extensive interface between the metal and the oxide phase. The oxidation of 10 mL MB (100 mg L^{-1}) with H_2O_2 (0.3 mol L^{-1}) at pH 6 with 30 mg of the catalyst produced a very rapid MB discoloration and 75 % TOC removal after 2 h of reaction. The studies suggest that the reactions proceed via $HO^{\bullet}$ generated from $Fe^{2+}{}_{surf}$ species and H_2O_2 in a Fenton-like mechanism. A simple mechanism for the oxidation of organic compounds is outlined in Figure 7. An efficient electron transfer from the Fe(0)/Fe_3O_4 composite to H_2O_2 takes place, with the formation of $HO^{\bullet}$, reinforced by the formation of very reactive small particle size Fe(0) and Fe_3O_4 with increased reactivity towards electron transfer reactions.

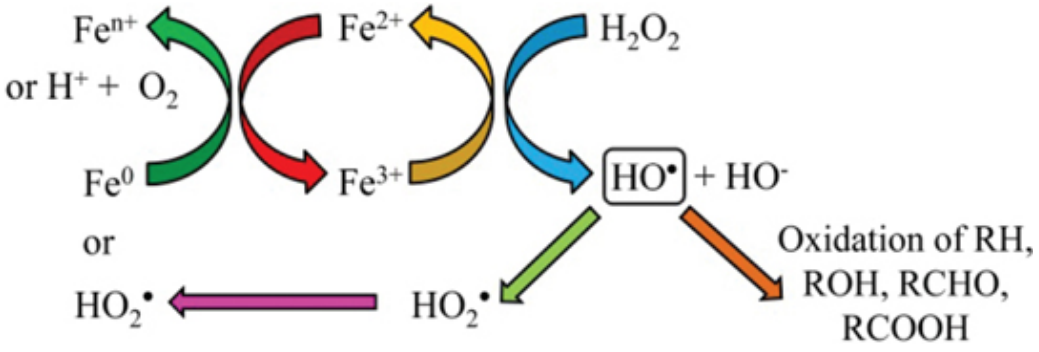

Figure 7: Simple mechanism for $HO^{\bullet}$ generation in the Fe(0)/Fe_3O_4 samples (adapted from reference [124].

Heterogeneous Fenton-like catalysts with iron modified with Pt, prepared from Pt(II) acetylacetonate and $Fe(CO)_5$, have been used in MB discoloration, and their performance was compared with that of Fe_3O_4 nanoparticles. Both FePt and Fe_3O_4 exhibited high activity toward MB discoloration (5 mg L^{-1}, pH 5.5, 3.5 % H_2O_2, 1 to 5 ppm of FePt NP). After 90 min reaction, the absorbance maximum near 665 nm of MB decreased by 26 % and 90 % for the 1 and 5 ppm solutions, respectively. The pseudo-first-order reaction rate constant for 5 ppm FePt nanoparticles was approximately 100 times faster than that obtained when using 5 ppm Fe_3O_4 nanoparticles under identical conditions. Furthermore, a concentration of 2500 ppm Fe_3O_4 was required to achieve the same reaction extent as 5 ppm FePt. The authors claim that an advantage of the use of these materials is that both FePt

and Fe_3O_4 NPs are superparamagnetic and can be easily separated with a magnet and reused for subsequent catalytic cycles [126].

A series of nanocomposites consisting of nZVI encapsulated in SiO_2 microspheres showed an excellent performance for MB degradation (10–16 mg L^{-1}) in the presence of H_2O_2. The MB degradation with the nanocomposite with the highest iron content (19.2 %) and 5 mL L^{-1} H_2O_2 was almost complete after 24 h treatment. The nanocomposites could be magnetically separated from the treated MB solution [127].

1.5 Heterogeneous Fenton reactions using modified iron nanoparticles prepared from natural plants

Although nanoparticles of iron oxides are very much used in solid Fenton reactions, the huge number of works performed on the subject makes impossible their inclusion in this review. However, as said, synthesis of nanoparticles from iron salts and natural leaves or grains of plants appears as advantageous due to their novelty and low cost. Therefore, we will shortly review the use of these materials on Fenton processes (only nanoparticles plus H_2O_2 addition).

Nanoparticles (claimed to be composed of zerovalent iron) obtained by a green single-step synthesis using green tea (GT, *Camellia sinensis*) and $FeCl_3$ (GT-nZVI) were used for bromothymol blue (BB) treatment in the presence of H_2O_2. The reaction of BB (500 mg L^{-1}) with GT-nZVI at different concentrations (0.03, 0.06, 0.12 and 0.33 mM) and adding 2 % H_2O_2 at pH 6 was effective for BB degradation; 0.33 mM GT-nZVI yielded the fastest degradation, with around 85 % removal in 15 min reaction time [118]. A similar result but with lower efficiency was obtained by using nanoparticles synthesized from aqueous sorghum (*Sorghum* spp.) extracts under the same conditions, yielding 60 % degradation after 30 min with 0.33 mM of nanoparticles, although the yield increased to 90 % when 0.66 mM NPs were used [119].

Shahwan et al. [128] synthesized iron materials from $FeCl_2{\cdot}4H_2O$ and GT, and determined that they consisted mainly of iron oxide/oxohydroxide nanoparticles. When 50.0 mg of these nanoparticles were added to solutions containing 5.0 mL of 10 % H_2O_2 and 45 mL of 50 mg L^{-1} MB solution at pH around 8, the removal of the dye proceeded almost instantaneously, with more than 80 % being removed within the first 5 min. Comparatively, the removal of methyl orange (MO) was slower, with 80 % of the dye being degraded after about 1 h of operation. Almost complete removal was achieved in 200 and 350 min for MB and MO, respectively. The same experiments but with iron nanoparticles synthesized using the conventional borohydride method, i. e., composed of Fe(0), gave a slightly lower efficiency for MB removal and significantly lower results in the case of MO.

Kuang et al. [129] tested iron nanoparticles prepared from three different tea extracts, GT, oolong tea (OT) and black tea (BT), for their capacity as catalysts for oxidation of monochlorobenzene (MCB, 50 mg L^{-1}). GT nanoparticles were able to remove 69 % of MCB at pH 6.1 followed by 53 % by particles prepared from OT and 39 % by those prepared from BT in 180 min, using [NPs] = 0.4 g L^{-1} and [H_2O_2] = 0.0894 M. With GT nanoparticles, i. e., the most efficient, and under the optimum experimental conditions (0.6 g L^{-1} NPs, 0.045 M H_2O_2, and pH 3), the material was able to oxidatively degrade 81 % of MCB along with a 31 % COD reduction in 180 min.

Machado et al. [130] tested nanoparticles synthesized using Fe(III) and grape marc, BT, and vine leaf extracts, for their degradation efficiency against ibuprofen, finding an enhancement of the reaction when H_2O_2 was added to the system. Here, it was not indicated if these NPs were composed of Fe(0) or iron oxides. For ibuprofen at 10 mg L^{-1}, 40–200 µL amounts of 3 % H_2O_2 and 30 mL of iron extract were incorporated. Samples of soils (50 g) contaminated with ibuprofen (2.8 mg kg^{-1}) were mixed with 10 mL of the iron extract, and different amounts of 3 % H_2O_2 (60–240 µL) were added in order to promote the Fenton reaction. The degradation process in sandy soil was slower than that in aqueous solution due to the time required for percolation. The combination of these nanoparticles in a Fenton reaction showed improved efficiency up to 95 % [131].

In another paper, GT nanoparticles prepared like in reference [119] were used for oxidation of malachite green (MG). When 0.74 g L^{-1} GT nanoparticles and 7.4 mM H_2O_2 were added to 250 mL of MG solution (50 mg L^{-1}), a very rapid degradation was obtained in few minutes (around 80 %), with low temperature effect (25–45 °C and [H_2O_2] (1–15 mM). The degradation efficiency declined slightly as the NPs dosage increased (0.3–1.1 g L^{-1}). Changes on pH (3–7) produced very few differences on MG removal, with the conclusion that the heterogeneous Fenton-like oxidation of MG using these NPs can occur over a wide pH range. *p*-Dimethylaminobenzaldehyde was identified as a product of MG degradation [132].

1.6 Supported nanoparticles as Fenton catalysts

As said before, one of the problems of the use of nZVI is the instability of the nanoparticles, as they aggregate and transform rapidly in water (Figure 5). A strategy to avoid this undesired aggregation is the immobilization in adequate supports, which also allows the recovery of the material after use and impedes its passage to water.

nZVI supported on NaY zeolite (nZVI/NaY) was synthesized by *in-situ* reduction of Fe^{2+}-exchanged NaY zeolite. 50–100 nm spherical nZVI particles supported on the surface of NaY have been obtained, as shown by TEM analysis. Composition and structural characterization showed that α-Fe nanoparticles (50–100 nm) were supported on the surface of the zeolite at a loading of Fe^{2+} around 2 wt%. This material was compared with unsupported nZVI (spherical particles, average diameter of about 80 nm) and with the CFP for the degradation of potassium hemiphthalate (KHP, 425 mg L^{-1}) [133]. The experiments were performed with a KHP solution (500 mg L^{-1} COD), 30 mM H_2O_2 and 1.5 mM iron at pH 3.5. The catalytic activity of nZVI/NaY was close to that of the homogeneous CFP but with less than 50 % leaching of iron cations; it also performed well under a much wider pH range (pH 1.7–5). The concentration of Fe^{2+} ions in solution was higher when using nZVI/NaY compared with nZVI (around 23 and 18 % of total iron content, respectively), attributed to the ability of nZVI/NaY to reduce Fe^{3+} to Fe^{2+}. At an initial pH of 1.7, 90 % COD reduction was achieved, while at pH 5 the COD decrease was 60 %. Upon three reuses at initial pH 3.5, the catalyst activity decreased from ca. 80 to 61 % COD removal.

Trinitroglycerin (TNG), a chemical used in the manufacture of dynamite, was degraded by using nZVI free and supported on the surface of nanostructured silica SBA-15 (Santa Barbara Amorphous No. 15), an inert polymer. ZVINs/SBA-15 nanoassembly was prepared by treating SBA-15 with $FeSO_4{\cdot}7H_2O$, followed by $NaBH_4$ reduction. Batch degradation experiments were performed at different pH values under Ar or air in 20 mL serum bottles, at which 10 mL of TNG solution (3.5 μmol) and the equivalent of unstabilized or stabilized nZVI (0.5 g L^{-1}) were added. Both nZVI and nZVI/SBA-15 degraded completely TNG in short times (5–15 min), producing glycerol and ammonium, but the reaction was faster with nZVI/SBA-15, which retained its original efficiency after five successive cycles [134].

1.7 PhotoFenton

The first examples of the use of the combination of UV radiation with H_2O_2 and solid iron materials have been performed by Doong and Chang [135, 136] for degradation of organophosphorous pesticides (OPPs) such as parathion, methamidophos, malathion, diazion, phorate and ethyl O-(*p*-nitrophenyl) phenylphosphonothionate (EPN). They treated 10 mg L^{-1} OPP, with 20 mg L^{-1} H_2O_2 and 1 g L^{-1} ZVI (> 99.5 % purity) or 50 μM ferrous ion at pH 7 under UV irradiation (100 W medium pressure mercury lamp, quartz photoreactor). There was no significant difference in the degradation rate between the UV/Fe(0)/H_2O_2 and the UV/Fe^{2+}/H_2O_2 systems. The order of reactivity of OPPs was phorate > methamidophos > EPN > diazion > malathion. In the case of parathion, diethylphosphoric acid, *p*-nitrophenol, diethylmonothiophosphoric acid, O,O-ethyl-*p*-nitrophenyl monothiophosphoric acid and oxalate were identified as intermediates, which shown to be oxidized further.

Application of Fenton and photoFenton type processes, UV/Fe^{2+}/H_2O_2 and UV/Fe(0)/H_2O_2, to the treatment of a dye wastewater was investigated. For this, the destruction of a model azo dye, C.I. Acid Orange 7 (AO7, 20 mg L^{-1}), was studied under different conditions, monitoring the discoloration and mineralization extent. First, the Fe^{2+}/H_2O_2 and Fe(0)/H_2O_2 dark Fenton processes were optimized in terms of the iron catalyst concentration and the iron catalyst/H_2O_2 ratio. The highest mineralization extent, 34.67 % of TOC removal after 60 min was achieved with [Fe^{2+}] = 1.0 mM and Fe^{2+}/H_2O_2 = 1:40. A higher value, 39.78 %, was obtained in the case of [Fe(0)] = 0.5 mM and Fe(0)/H_2O_2 ratio of 1:20, i. e. 5.21 % higher in comparison with that achieved by Fe^{2+}/H_2O_2, although the concentration of iron catalyst was lower. Systems at those optimal conditions were combined with UV-C radiation (125 W mercury lamp, 254 nm) to test an enhancement of dye degradation. All processes have shown high efficiency for bleaching of the model dye solution, with complete discoloration in all cases. More than 95 % of color removal was obtained in the UV/Fe^{2+}/H_2O_2 process almost immediately, while the complete bleaching was achieved after 20 min of reaction time. It was suggested that UV light was able to degrade Fe-complexes formed between iron and organic species, yielding a higher discoloration. AO7 mineralization by both Fe^{2+}/H_2O_2 and Fe(0)/H_2O_2 processes was significantly enhanced in the presence of UV irradiation, from 34.67 up to 84.12 % and from 39.78 to 90.09 % of removed TOC, respectively [137].

Devi et al. [138] investigated a photoFenton process to degrade Alizarin Red S anthraquinone dye (ARS). ARS degradation was investigated by using ZVI in powder (95 % purity, 300-mesh size, electrolytic) with H_2O_2. For irradiation, a 125 W medium pressure mercury vapor lamp was used. The best conditions, evaluated through rate constants, were: [ARS] = 200 mg L^{-1}, [ZVI] = 50 mg L^{-1} and [H_2O_2] = 100 mg L^{-1} at pH 3.

A photoFenton like method using commercial nZVI combined by UV and H_2O_2 was applied for removing total petroleum hydrocarbons (TPH) from a gas station diesel fuel in a water-oil emulsion using sodium dodecyl sulfate (SDS) [139]. An optimal removal between 95 % and 100 % was achieved. The nZVI particles can be reused in a magnetic field. This process may enhance the rate of diesel degradation in polluted water and could be used as a pretreatment step for the biological removal of TPH from diesel fuel in the aqueous phase. The influence of different parameters on TPH reduction rate including the initial TPH concentration (0.1–1 mg L^{-1}), H_2O_2 concentration (5–20 mM), nZVI concentration (10–100 mg L^{-1}), pH (3–9), and reaction time (15–120 min) were in-

vestigated. A variance analysis suggested that the optimal conditions were: $[TPH]_0 = 0.7\ mg\ L^{-1}$, [nZVI] = 20 mg L^{-1}, $[H_2O_2] = 5\ mM$, pH 3, 60 min. The predicted removal rate in the optimal conditions was 95.8 %, what was confirmed by the obtained data (95–100 %).

2 Conclusions

Homogeneous Fenton processes in their various types have been extensively studied and applied in remediation processes. The processes are cost effective, the reagents are easily available and the systems can be efficiently scaled up for practical applications. However, the need of acid pH through further neutralization and the removal of iron ions at the end of the treatment are costly and require technical operation and maintenance. Thus, the use of zerovalent iron, either macro-, micro- o nanosized, allows to reduce the concentration of iron ions in the treated water, with the possibility of extending the working pH range.

Remediation with zerovalent iron is rapidly growing for application in several sites and effluents, and many evidences have proven that Fe(0) is a highly efficient and affordable material. In recent years, the focus was mainly directed on the use of nanoscale Fe(0).

Due to the chemical and physical structures of ZVI and nZVI, this type of materials are very promising to develop heterogeneous catalysts of high activity, especially in the case of nZVI due to the high specific surface area and the improved catalytic activity. However, considerable performance improvement is still pending due to unsatisfactory activity and efficiency, especially the tendency to agglomerate, loosing efficiency, and to undergo leaching with limited reusability.

The selection of ZVI as solid catalysts must fulfill requirements of a high activity, marginal leaching of active cations, stability over a wide range of pH and temperature, and a high H_2O_2 conversion with minimum decomposition. Last but not least, the materials should be available at a reasonable cost.

The combination of ZVI or nZVI with H_2O_2 in an AFP needs, as in the case of CFP, especial conditions of pH, temperature and amount of H_2O_2 for optimization. Comparing the particle size, nZVI systems present a clear advantage over ZVI systems in terms of H_2O_2 consumption. However, nZVI systems do not exhibit excellent reusability results because of a rapid oxidation of iron nanoparticles within the experimental duration in the presence of H_2O_2. In contrast, ZVI can be reused for numerous cycles of reaction.

Additionally, the development of processes combining a Fenton treatment with further biological methods, or the pretreatment with nZVI followed by H_2O_2 addition are possible routes to improve the removal of recalcitrant pollutants.

Summarizing, big efforts should be done to advance and adapt this technology for water and soil treatment, combining the studies with fundamental work for thorough understanding of the mechanisms and kinetic aspects related to the systems.

References

1. Oliveros E, Legrini O, Hohl M, Miller T, Braun AM. Chem Eng Process. 1997;36:397–405.
2. Hug SJ, Leupin O. Environ Sci Technol. 2003;37:2734–2742.
3. Hug SJ, Ulrichlaubscher H. Environ Sci Technol. 1997;31:160–170.
4. Fenton HJH. J Chem Soc. 1894;65:899–910.
5. Barbusiński K. Ecol Chem Eng S. 2009;16:347–358.
6. Babuponnusami A, Muthukumar K. J Environ Chem Eng. 2014;2:557–572.
7. Casero I, Sicilia D, Rubio S, Pérez-Bendito D. Water Res. 1997;31:1985–1995.
8. Kuo WG. Wat Res. 1992;26:881–886.
9. Nam S, Renganathan V, Tratnyek PG. Chemosphere. 2001;45:59–65.
10. Barbusiński K. Polish J Environ Stud. 2005;14:281–285.
11. Huston PL, Pignatello JJ. Water Res. 1999;33:1238–1246.
12. Barbusiński K, Filipek K. Polish J Environ Stud. 2001;10:207–212.
13. Ikehata K, Gamal El-Din MJ. Environ Eng Sci. 2006;5:81–135.
14. Lin SH, Lin CM, Leu HG. Water Res. 1999;33:1735–1741.
15. Kitis M, Adams CD, Daigger GT. Water Res. 1999;33:2561–2568.
16. Perkowski J, Jóźwiak W, Kos L, Stajszczyk P. Fibres Text East Eur. 2006;14:114–119.
17. Ming-Jer L, Ming-Chun L, Jong-Nan C. Water Res. 2003;37:3172–3179.
18. Pignatello JJ, Oliveros E, MacKay A. Crit Rev Env Sci Tech. 2006;36:1–84.
19. Rivas FJ, Beltran FJ, Frades J, Buxeda P. Water Res. 2001;35:387–396.
20. Lin SH, Lo CC. Water Res. 1997;31:2050–2056.

21. Pignatello JJ, Liu D, Huston P. Environ Sci Technol. 1999;33:1832–1839.
22. Haber F, Weiss J. Proc Roy Soc. 1934;147:332–351.
23. Barb WG, Baxendale JH, George P, Hargrave KR. Trans Faraday Soc. 1951;47:462–500.
24. Barb WG, Baxendale JH, George P, Hargrave KR. Trans Faraday Soc. 1951;47:591–616.
25. Walling C. Acc Chem Res. 1975;8:125–131.
26. Kremer ML, Stein G. Trans Faraday Soc. 1959;55:959–973.
27. Kremer ML. Trans Faraday Soc. 1962;58:702–707.
28. Kremer ML, Stein G. Int J Chem Kinet. 1977;9:179–184.
29. Sutton HC, Winterbourn CC. Free Radical Biol Med. 1989;6:53–60.
30. Kremer ML. Phys Chem Chem Phys. 1999;1:3595–3605.
31. Kremer ML. J Phys Chem A. 2003;107:1734–1741.
32. Bray WC, Gorin MH. J Am Chem Soc. 1932;54:2124.
33. Ensing B, Buda F, Bloechl P, Baerends E. J Angew Chem Int Ed. 2001;40:2893–2895.
34. Ensing B, Buda F, Bloechl P, Baerends E. Phys Chem Chem Phys. 2002;4:3619–3627.
35. Mignon P, Pera Titus M, Chermette H. Phys Chem Chem Phys. 2012;14:3766–3774.
36. Jacobsen F, Holcman J, Sehested K. Int J Chem Kinet. 1998;30:215–221.
37. Gallard H, De Laat J, Legube B. Wat Res. 1999;33:2929–2936.
38. Salgado P, Melin V, Contreras D, Moreno Y, Mansilla HD. J Chil Chem Soc. 2013;58:2096–2101.
39. Bossmann SH, Oliveros E, Göb S, Siegwart S, Dahlen EP, Payawan L, et al. J Phys Chem A. 1998;102:5542–5550.
40. Mukherjee R, Kumar R, Sinha A, Lama Y. Crit Rev Env Sci Tech. 2016;46:443–466.
41. Iurascu B, Siminiceanu J, Vione D, Vicente MA, Gil A. Water Res. 2009;43:1313–1322.
42. Eisenhauer HRJ. Water Pollut Control Fed. 1964;36:1116–1128.
43. Ma YS, Huang ST, Lin JG. Water Sci Technol. 2000;42:155–160.
44. Babuponnusami A, Muthukumar K. Clean-Soil Air Water. 2011;39:142–147.
45. Kavitha V, Palanivelu K. Water Res. 2005;39:3062–3072.
46. Xu XR, Li XY, Li XZ, Li HB. Sep Purif Technol. 2009;68:261–266.
47. Kwon BG, Lee DS, Kang N, Yoon J. Water Res. 1999;33:2110–2118.
48. Szpyrkowicz L, Juzzolino C, Kaul SN. Water Res. 2001;35:2129–2136.
49. Parsons S. Advanced oxidation processes for water and wastewater treatment. London: IWA Publishing, 2004.
50. Faust BC, Hoigne J. Atmos Environ. 1990;24:79–89.
51. Bauer R, Fallmann H. Res Chem Intermed. 1997;23:341–354.
52. Bauer R, Waldner G, Fallmann H, Hager S, Klare M, Krutzler T, et al. Catal Today. 1999;53:131–144.
53. Pliego G, Zazo JA, Garcia-Muñoz P, Munoz M, Casas JA, Rodriguez JJ. Crit Rev Env Sci Technol. 2015;45:2611–2692.
54. Pouran SR, Aziz ARA, Daud WMAW. J Ind Eng Chem. 2015;21:53–69.
55. Ortega-Liébana MC, Sánchez-López E, Hidalgo-Carrillo J, Marinas A, Marinas JM, Urbano FJ. Appl Catal B Environ. 2012;127:316–322.
56. Zepp RG, Faust BC, Hoigné J. Environ Sci Technol. 1992;26:313–319.
57. Safarzadeh-Amiri A, Bolton JR, Cater SR. Water Res. 1997;31:787–798.
58. De Oliveira IS, Viana L, Verona C, Fallavena VLV, Azevedo CMN, Pires M. J Hazard Mater. 2007;146:564–568.
59. Hermosilla D, Cortijo M, Huang CP. Sci Total Environ. 2009;407:3473–3481.
60. Ruppert G, Bauer R, Heisler G. J Photochem Photobiol A. 1993;73:75–78.
61. Sun Y, Pignatello JJ. Environ Sci Technol. 1993;27:304–310.
62. Gogate PR, Pandit AB. Adv Environ Res. 2004;8:553–597.
63. Zepp RG, Faust BC, Hoigne J. Environ Sci Technol. 1992;26:313–319.
64. McGinnis BD, Adams VD, Middlebrooks EJ. Water Res. 2000;34:2346–2354.
65. Kim SM, Geissen SU, Vogelpohl A. Water Sci Technol. 1997;35:239–248.
66. Legrini O, Oliveros E, Braun AM. Chem Rev. 1993;93:671–698.
67. Southworth BA, Voelker BM. Environ Sci Technol. 2003;37:1130–1136.
68. Tang WZ, Chen RZ. Chemosphere. 1996;32:947–958.
69. Fajerwerg K, Debellefontaine H. Appl Catal B. 1996;10 L229–L235.
70. Pera-Titus M, García-Molina V, Baños MA, Giménez J, Esplugas S. Appl Catal B. 2004;47:219–256.
71. Li R, Zhang L, Wang P. Nanoscale. 2015;7:17167–17194.
72. Navalon S, Alvaro M, Garcia H. Appl Catal B. 2010;99:1–26.
73. Zhao X, Liu W, Cai Z, Han B, Qian T, Zhao D. Water Res. 2016;100:245–266.
74. Dhakshinamoorthy A, Navalon S, Alvaro M, Garcia H. Chem Sus Chem. 2012;5:46–64.
75. Weiss J. Trans Faraday Soc. 1935;31:1547–1557.
76. Powell RM, Puls RW, Hightower SK, Sabatini DA. Environ Sci Technol. 1995;29:1913–1922.
77. Warren KD, Arnold RG, Bishop TL, Lindholm LG, Betterton EA. J Hazard Mater. 1995;41:217–227.
78. Ghauch A. Freiberg Online Geoscience. 2015;38:1–80.
79. Noubactep C. Environ Technol. 2008;29:909–920.
80. Guan X, Sun Y, Qin H, Li J, Lo IMC, He D, et al. Water Res. 2015;75:224–248.
81. Bremner DH, Burgess AE, Houllemare D, Namkung K-C. Appl Catal B. 2006;63:15–19.
82. Fu F, Dionysiou DD, Liu H. J Hazard Mater. 2014;267:194–205.
83. Segura Y, Martinez F, Melero JA. Appl Catal B. 2013;136–137:64–69.
84. Keenan CR, Sedlak DL. Environ Sci Technol. 2008;42:1262–1267.
85. Keenan CR, Sedlak DL. Environ Sci Technol. 2008;42:6936–6941.

86. Bremner DH, Burgess AE. (2004). Patent US 6692632University of Abertay Dundee.
87. Namkung KC, Burgess AE, Bremner DH. Environ Technol. 2005;26:341–352.
88. Wada H, Naoi T, Homma T. J Jpn Soc Water Environ. 1993;16:892–897.
89. Takemura Y, Seno-O K, Mukai T, Suzzuki M. Water Sci Technol. 1994;30:129–137.
90. Lücking F, Koser H, Jank M, Ritter A. Water Res. 1998;32:2607–2614.
91. Zhou T, Li Y, Ji J, Wong F-S, Lu X. Sep Purif Technol. 2008;62:551–558.
92. Kallel K, Belaid C, Mechichi T, Ksibi M, Elleuch B. Chem Eng J. 2009;150:391–395.
93. Özdemir C, Tezcan H, Sahinkaya S, Kalipci E. Clean Soil Air Water. 2010;38:1152–1158.
94. Cabrera LC, Caldas SS, Rodrigues S, Bianchini A, Duarte FA, Primel EG. J Braz Chem Soc. 2010;21:2347–2352.
95. Fu FL, Wang Q, Tang B. J Hazard Mater. 2010;174:17–22.
96. Chu LB, Wang JL, Dong J, Liu HY, Sun XL. Chemosphere. 2012;86:409–414.
97. Arienzo M. Chemosphere. 2000;40:441–448.
98. Liao C-J, Chung T-L, Chen W-L, Kuo S-L. J Mol Catal A Chem. 2007;265:189–194.
99. Barreto-Rodrigues M, Silva FT, Paiva TCB. J Hazard Mater. 2009;168:1065–1069.
100. Jiang BC, Lu ZY, Liu FQ, Li AM, Dai JJ, Xu L, et al. Chem Eng J. 2011;174:258–265.
101. Le C, Liang J, Wu J, Li P, Wang X, Zhu N, et al. Water Sci Technol. 2011;64:2126–2131.
102. Shen J, Ou C, Zhou Z, Chen J, Fang K, Sun X, et al. J Hazard Mater. 2013;260:993–1000.
103. Kharisov BI, Kharissova OV, Rasika Dias HV, Ortiz Méndez U, Gómez De La Fuente I, Peña Y, Norena LE, Wang J-A. Iron-based Nanomaterials in the Catalysis. Rijeka: Intech, 2016:35–68.
104. Crane RA, Scott TB. J Hazard Mater. 2012;211–212:112–125.
105. Noubactep C, Caré S. J Hazard Mater. 2010;182:923–927.
106. Sun Y-P, Li X-Q, Cao J, Zhang W-X, Wang HP. Adv Colloid Interface Sci. 2006;120:47–56.
107. Mukherjee R, Kumar R, Sinha A, Lama Y, Saha AK. Crit Rev Env Sci Technol. 2016;46:443–466.
108. Corrias A, Ennas G, Licheri G, Marongiu G, Paschina G. Chem Mater. 1990;2:363–366.
109. Glavee GN, Klabunde KJ, Sorensen CM, Hadjipanayis GC. Inorg Chem. 1995;34:28–35.
110. Wang CB, Zhang WX. Environ Sci Technol. 1997;31:2154–2156.
111. Li F, Vipulanandan C, Mohanty KK. Colloids Surf A. 2003;223:103–112.
112. Suslick KS, Fang M, Hyeon T. J Am Chem Soc. 1996;118:11960–11961.
113. van Wonterghem J, Mørup S, Koch CJ, Charles SW, Wells S. Nature. 1986;322:622–623.
114. Yoo B-Y, Hernandez SC, Koo B, Rheem Y, Myung NV. Water Sci Technol. 2007;55:149–156.
115. Kataby G, Ulman A, Prozorov R, Gedanken A. Langmuir. 1998;14:1512–1515.
116. Zaera FA. J Vac Sci Tech. 1989;A7:640–645.
117. Li S, Yan W, Zhang WX. Green Chem. 2009;11:1618–1626.
118. Hoag GE, Collins JB, Holcomb JL, Hoag JR, Nadagouda MN, Varma RS. J Mater Chem. 2009;19:8671–8677.
119. Njagi EC, Huang H, Stafford L, Genuino H, Galindo HM, Collins JB, et al. Langmuir. 2010;27:264–271.
120. Babuponnusami A, Muthukumar K. Separ Purif Technol. 2012;98:130–135.
121. Joo SH, Feitz AJ, Waite TD. Environ Sci Technol. 2004;38:2242–2247.
122. Xu L, Wang J. J Hazard Mater. 2011;186:256–264.
123. Bergendahl JA, Thies TP. Water Res. 2004;38:327–334.
124. Moura FCC, Araujo MH, Costa RCC, Fabris JD, Ardisson JD, Macedo WAA, et al. Chemosphere. 2005;60:1118–1123.
125. Costa RCC, Moura FCC, Ardisson JD, Fabris JD, Lago RM. Appl Catal B. 2008;83:131–139.
126. Hsieh S, Lin P-Y. J Nanopart Res. 2012;14:956–965.
127. Mao Z, Wu Q, Wang M, Yang Y, Long J, Chen X. Nanoscale Res Lett. 2014;9:501–509.
128. Shahwan T, Abu Sirriah S, Nairat M, Boyaci E, Eroğlu AE, Scott TB, et al. Chem Eng J. 2011;172:258–266.
129. Kuang Y, Wang Q, Chen Z, Megharaj M, Naidu R. J Colloid Interface Sci. 2013;410:67–73.
130. Machado S, Pinto SL, Grosso JP, Nouws HPA, Albergaria JT, Delerue-Matos C. Sci Total Environ. 2013;445–446:1–8.
131. Machado S, Stawiński W, Slonina P, Pinto AR, Grosso JP, Nouws HP, et al. Sci Total Environ. 2013;461–462:323–329.
132. Wu Y, Zeng S, Wang F, Megharaj M, Naidu R, Chen Z. Sep Purif Technol. 2015;154:161–167.
133. Wang W, Zhou M, Mao Q, Yue J, Wang X. Catal Commun. 2010;11:937–941.
134. Saad R, Thiboutot S, Ampleman G, Dashan W, Hawari J. Chemosphere. 2010;81:853–858.
135. Doong R-A, Chang W-H. J Photochem Photobiol A. 1998;116:221–228.
136. Doong R, Chang W. Chemosphere. 1998;37:2563–2572.
137. Kusic H, Koprivanac N, Srsan L. J Photochem Photobiol A. 2006;181:195–202.
138. Devi LG, Rajashekhar KE, Raju KSA, Kumar SG. J Mol Catal A Chem. 2009;314:88–94.
139. Dehghani M, Shahsavani E, Farzadkia M, Reza Samaei M. J Environ Health Sci Eng. 2014;12:87–93.